

## Exploring the differences between BRCA mutated and HRwild-type high grade serous ovarian cancer: A multiomic analysis

Ayesha B. Alvero<sup>a,d</sup>, Sharon Wu<sup>b</sup>, Alex Farrell<sup>b</sup>, Seongho Kim<sup>c</sup>, John J. Wallbillich<sup>d</sup>, Ira Winer<sup>d</sup>, Robert Morris<sup>d</sup>, David Spetzler<sup>b</sup>, Matthew L. Anderson<sup>e</sup>, Alberto Puccini<sup>f,g</sup>, Nathaniel L. Jones<sup>h</sup>, Thomas J. Herzog<sup>i</sup>, Premal H. Thaker<sup>j</sup>, Gil Mor<sup>a,d</sup>, Radhika P. Gogoi<sup>d,\*</sup>

<sup>a</sup> C.S. Mott Center for Human Growth and Development, Department of Obstetrics and Gynecology, Wayne State University, Detroit, MI, United States of America

<sup>b</sup> Caris Life Sciences, Tempe, AZ, United States of America

<sup>c</sup> Department of Oncology, Biostatistics and Bioinformatics Core, Karmanos Cancer Institute, Detroit, MI, United States of America

<sup>d</sup> Karmanos Cancer Institute/ Wayne State University, Detroit, MI, United States of America

<sup>e</sup> Department of Obstetrics and Gynecology, University of South Florida, Tampa, FL, United States of America

<sup>f</sup> Department of Biomedical Sciences, Pieve Emanuele, Humanitas University, Milan, Italy

<sup>g</sup> Medical Oncology and Hematology Unit, Humanitas Cancer Center, IRCCS Humanitas Research Hospital, Rozzano, Milan, Italy

<sup>h</sup> Mitchell Cancer Institute, Division of Gynecologic Oncology, University of South Alabama, United States of America

<sup>i</sup> Univ of Cincinnati Cancer Center & Dept of Ob/Gyn, Division of Gyn Oncology, Cincinnati, OH, United States of America

<sup>j</sup> Division of Gynecologic Oncology, Washington University School of Medicine and Siteman Cancer Center, St Louis, MO, United States of America

### HIGHLIGHTS

- We present transcriptomic analysis of the largest set of BRCA1 and 2-mut high grade serous ovarian cancer (HGSOC).
- BRCA-mut and HR wild-type HGSOC have different levels of amplification of CCNE1, AKT2 and ERBB2.
- BRCA1-mut, BRCA2-mut and HRwt HGSOC have difference in immune-relayed pathways and immune checkpoint gene expression.
- BRCA1-mut HGSOC have higher NKT cell infiltration, higher T-cell inflamed and IFN $\gamma$  scores.

### ARTICLE INFO

#### Article history:

Received 13 December 2024

Received in revised form 7 February 2025

Accepted 8 February 2025

Available online xxx

#### Keywords:

High grade serous ovarian carcinoma

BRCA1

BRCA2

Tumor immune microenvironment

### ABSTRACT

**Objective.** The purpose of this study was to evaluate the transcriptomic profile of BRCA1 mutant (BRCA1mut) and BRCA2 mutant (BRCA2mut) HGSOC compared to homologous recombination wild-type (HRwt) tumors utilizing the CARIS database.

**Methods.** Next-generation and Whole Transcriptome Sequencing (WTS; Caris Life Sciences, Phoenix, AZ) was performed on a total of 2745 HGSOC tumor samples. BRCA mutations were defined as variants resulting in loss-of-function of the protein and HRwt was defined as samples wildtype for aberrations in both BRCA1 and BRCA2, as well as for 28 other HR genes. HRwt group was further classified into HRwt/LOH-low (<16%) and HRwt/LOH-high ( $\geq$ 16%). Genomic analysis consists of mutation analysis and measurements of TMB and MSI. Transcriptomic analysis included identification of Differentially expressed genes (DEGs), GSEA and immune deconvolution.

**Results.** We identified 519 (19%) BRCA1-mut, 302 (11%) BRCA2-mut, and 739 (27%) HRwt/LOH high and 1181 (43%) HRwt/LOH low HGSOC. *TP53* was the most commonly mutated gene in all groups. Mutations in *PIK3CA* were most common in HRwt/LOH-low compared to BRCA1-mut and BRCA2-mut HGSOC. TMB-H was highest in BRCA2-mut compared to BRCA1-mut, HRwt/LOH high and HRwt/LOH low tumors. In contrast, higher NKT cell infiltration, higher T cell inflamed and IFN $\gamma$  scores, and higher PDL1 expression were observed in BRCA1-mut tumors.

**Conclusion.** Our findings emphasize the differential immune profiles based on BRCA1 and BRCA2 mutations and suggest potential therapeutic targets, including treatment strategies that incorporate immunotherapy and target specific genomic alterations.

© 2025 The Authors. Published by Elsevier Inc. This is an open access article under the CC BY-NC-ND license (<http://creativecommons.org/licenses/by-nc-nd/4.0/>).

\* Corresponding author at: 4100 John R Street HP07GO, Detroit, MI 48201, United States of America.

E-mail address: [Radhikagogoi@wayne.edu](mailto:Radhikagogoi@wayne.edu) (R.P. Gogoi).

## 1. Introduction

Eukaryotes protect the integrity of their genome through various DNA damage response (DDR) pathways. These include pathways for the repair of both single-strand breaks and double-strand breaks such as non-homologous end joining (NHEJ) and homologous recombination (HR) [1]. Mutations in genes in these pathways are frequently observed in cancers highlighting their importance in tumor suppression [2]. In particular, germline mutations in *BRCA1* or *BRCA2* genes are associated with a heritable susceptibility to breast, ovarian and other cancers in both men and women [3]. Specifically for ovarian cancer, somatic *BRCA1/2* mutations can be found in as many as 16 % to 21 % of high-grade serous ovarian cancer (HGSOC) [4–6].

*BRCA1* and *BRCA2* are crucial for repairing DNA double-strand breaks through HR. While *BRCA1* has a broad range of functions, including roles in HR, NHEJ, and cell cycle, *BRCA2* plays a more focused role by facilitating the localization of RAD51 to DNA double-strand breaks. Despite their shared involvement in HR, the distinct molecular functions of *BRCA1* and *BRCA2* lead to different cancer characteristics when these genes are mutated [7].

Both *BRCA1* and *BRCA2* mutations are linked to hereditary breast and ovarian cancers but affect disease characteristics differently. For instance, although the risk of breast cancer is similar for carriers of both mutations, *BRCA1*-mutated (*BRCA1-mut*) breast cancers are more likely to be triple-negative (i.e., lacking estrogen receptor, progesterone receptor, and HER2), a subtype that is generally more aggressive and challenging to treat. Additionally, individuals with pathogenic *BRCA1* mutations face a higher cumulative lifetime risk of developing HGSOC, approximately 50 %, compared to about 30 % for those with *BRCA2* mutations [3,8].

The impact on disease progression is also different. One of the key observations from studies of *BRCA1-mut* and *BRCA2-mut* ovarian cancers is their differential behavior not only when compared to tumors lacking these mutations but also when compared to each other. Specifically, subgroup analysis suggest that *BRCA2-mut* HGSOC demonstrate better overall survival (OS) and better response to chemotherapy compared to *BRCA1-mut* tumors [9,10].

Collectively, current studies indicate that *BRCA1* and *BRCA2* mutations have distinct effects on cancer susceptibility and outcomes. However, the precise pathways and genes through which these mutations exert their differential impacts are not well understood. This study aimed to bridge this knowledge gap by comparing transcriptome patterns in *BRCA1-mut* and *BRCA2-mut* HGSOC. We describe a unique immunological signature associated with these HGSOC tumors, which could explain their distinctive behavior. Gaining an understanding of these differences could lead to the development of targeted therapies tailored to *BRCA1* and *BRCA2* mutations, and potentially inform combinatorial strategies for HRwt tumors.

## 2. Materials and methods

### 2.1. Specimen profiling and clinical demographics

2745 HGSOC tumors were identified. Whole exome sequencing (WES) data was used to categorize these tumors as either *BRCA1-mut*, *BRCA2-mut* or HRwt. *BRCA1/2* mutations are somatic loss of function (LOF) mutations and HRwt status was defined as being WT for 30 DNA Damage response genes: *BRCA1*, *BRCA2*, *ATM*, *ATR*, *ATRX*, *BARD1*, *BLM*, *BRIP1*, *CHEK1*, *CHEK2*, *FANCA*, *FANCC*, *FANCD2*, *FANCE*, *FANCF*, *FANCG*, *FANCI*, *FANCL*, *FANCM*, *NBN*, *PALB2*, *RAD50*, *RAD51*, *RAD51B*, *RAD51C*, *RAD51D*, *RAD52*, *RAD54L*, *RPA1*, *MRE11*. Patients in the HRwt group were further subdivided into loss of heterozygosity (LOH) high/low status as described below. All samples were analyzed in a Clinical Laboratory Improvement Amendments/College of American Pathologists (CLIA/CAP)-certified laboratory (Caris Life Sciences, Phoenix, AZ). All patients with molecular data available in our database at the time

of analysis were included. A subset of the patients ( $n = 2070$ ) had available clinical outcomes data in the Caris CODEai database containing the results of somatic tumor profiling - WES and whole transcriptome (WTS) profiling by Next Generation Sequencing (NGS) performed for clinical indications by a single CLIA/CAP-certified laboratory (Caris Life Sciences, Phoenix, AZ).

Real-world OS information was obtained from insurance claims data from the Caris CODEai clinico-genomic database. OS was calculated from time of tissue collection (as a surrogate for diagnosis) to last contact, or from first treatment with Carboplatin until last contact. The distributions of OS were graphically summarized using Kaplan-Meier curves for molecularly defined patient cohorts. Significance was set at  $p < 0.05$ .

### 2.2. Manual microdissection for DNA and RNA profiling

Manual microdissection was used to enrich for cancer cells for downstream DNA and RNA sequencing. Briefly, hematoxylin and Eosin (H&E) slides of formalin-fixed paraffin-embedded (FFPE) tumors were reviewed by a pathologist. Slides were then stained with nuclear fast red and tumor area was manually dissected. A minimum of 10 % and 20 % tumor content in the area was required to enable enrichment and extraction of tumor-specific RNA and DNA, respectively. Tumor-associated immune cells were not excluded.

### 2.3. Genomic profiling

NGS using either the Caris NGS-592 targeted panel or the Caris Whole Exome Sequencing (WES) 720-boosted gene panel was performed on genomic DNA isolated from FFPE micro dissected tumor samples using the NextSeq or NovaSeq 6000 platforms (Illumina, Inc., San Diego, CA). Sample preparation and sequence alignment and downstream analysis as well as clinical interpretations of mutations were identical between NGS platforms. All variants were detected with >99 % confidence, with an average sequencing depth of coverage >500× and an analytic sensitivity of 5 %. Genetic variants identified were interpreted by board-certified molecular geneticists according to the American College of Medical Genetics and Genomics (ACMG) standards. For mutation frequencies, 'pathogenic,' and 'likely pathogenic' were counted as mutations while 'benign,' 'likely benign' variants and 'variants of unknown significance' were excluded. Variants detected were mapped to reference genome (hg19), and well-established bioinformatics tools such as BWA, SamTools, GATK, and snpFF were incorporated to perform variant calling functions; germline variants were filtered with various germline databases including 1000 Genomes and dbSNP.

TMB was measured by counting nonsynonymous missense mutations that had not been previously described as germline alterations. The threshold to define TMB-high was  $\geq 10$  mutations/MB.

MSI was examined using over 7000 target microsatellite loci and compared to reference genome hg19. Only insertions or deletions that increased or decreased the number of repeats were considered. The threshold to determine MSI by NGS was determined to be 46 or more loci with insertions or deletions.

### 2.4. LOH calculation

The 22 autosomal chromosomes were split into 552 segments, and the LOH of single nucleotide polymorphisms (SNPs) within each segment was calculated. The final call of genomic LOH was based on the % of all 552 segments with observed LOH (High  $\geq 16$  %, Low <16 %) [11].

### 2.5. Whole transcriptome sequencing (WTS) and analysis

Qiagen RNeasy FFPE Kit (Qiagen, 73,504) was used for RNA extraction. Biotinylated RNA baits were hybridized to the synthesized and

purified cDNA targets and the bait-target complexes were amplified in a post capture PCR reaction. The resultant libraries were quantified and normalized, and the pooled libraries were denatured, diluted, and sequenced using the Illumina Novaseq 6500 platform to an average of 60 M reads. Raw data was demultiplexed by Illumina Dragen BioIT accelerator, trimmed, counted, PCR-duplicates removed and aligned to human reference genome hg19 by STAR aligner. For transcription counting, transcripts per million (TPM) molecules was generated using the Salmon expression pipeline. Gene set enrichment analysis (GSEA, Broad Institute) using the Hallmarks of Cancer Pathways collection was used to determine pathway enrichment between groups [12].

## 2.6. Immune-related analyses

Relative abundance of immune cell infiltrates in the tumor microenvironment were calculated from WTS data using xCell. T cell inflamed scores were calculated using a 160-gene T cell inflamed gene expression signature. The score defines inflamed  $\geq 80$ , intermediate  $> -80$  to  $< 80$  and not inflamed  $\leq -80$  [13]. Interferon gamma (IFN $\gamma$ ) scores were calculated using a validated 18-gene signature [14].

## 2.7. Immunohistochemistry (IHC) analyses

FFPE sections were stained using automated techniques, which were optimized and validated per CLIA/CAP and ISO requirements. The primary antibodies for MLH1 and PMS2 were M1 and EPR3947 clones, respectively (Ventana Medical Systems, Inc., Tucson, AZ, USA); complete absence of expression was indicative of MMR deficiency (dMMR). The primary antibody used against PD-L1 was SP142 (Spring Biosciences), following the Caris Life Sciences laboratory developed test (LDT) for this antibody. Staining was scored for intensity (0 = no staining; 1+ = weak staining; 2+ = moderate staining; 3+ = strong staining) and staining percentage (0–100%). The staining was regarded as PD-L1 positive if its intensity on the membrane of the tumor cells was  $\geq 2+$  and the percentage of positively stained cells was  $> 5\%$ . A board-certified pathologist evaluated all IHC results independently.

## 2.8. Statistical analysis

Mann-Whitney U and chi-square tests were used to evaluate continuous and categorical molecular and immunological differences, respectively, between *BRCA1-mut*, *BRCA2-mut*, HRwt/LOH-low and HRwt/LOH-high groups, with multiple comparison correction (corrected  $q < 0.05$  was considered significant, and  $p < 0.05$  considered a trend) done by the Benjamini-Hochberg method.

## 2.9. Compliance statement

This study was conducted in accordance with guidelines of the Declaration of Helsinki, Belmont report, and U.S. Common rule. In keeping with 45 CFR 46.101(b)(4), this study is considered Institutional Review Board (IRB) exempt and no patient consent was necessary from the subject, as it was performed utilizing retrospective, deidentified clinical data.

## 3. Results

### 3.1. Description of study cohort

A total of 2745 HGSOC were identified. Of these, 519 (18.9%) were classified as *BRCA1-mut*, 302 (11%) were classified as *BRCA2-mut*, 4 (0.15%) were both *BRCA1-mut* and *BRCA2-mut*, and 1181 (43%) were independently categorized as HRwt/LOH-low and 739 (26.9%) as HRwt/LOH-high. Median age at biopsy collection for *BRCA1-mut* patients is significantly lower than other groups ( $q < 0.05$ ) (Supplemental

Table 1). For *BRCA1-mut* patients, the median age at biopsy collection was 59 years (range = 26–90), compared with 65 years (range = 24–90) for *BRCA2-mut* patients, 67 (range = 18–90) for HRwt/LOH-low, and 65 (range = 20–90) for HRwt/LOH-high. Interestingly, patients with mutations in both *BRCA1* and *BRCA2* had an even earlier age at diagnosis of 51.5 (range = 51–66). Fig. 1 outlines the analysis process for the study.

### 3.2. Clinical outcomes for genomically-defined subsets of HGSOC patients

To understand the clinical impact of specific genotypes on HGSOC outcomes, survival analyses were conducted to compare genomically-defined subsets of subjects. For this analysis, we compared *BRCA1-mut*, *BRCA2-mut*, HRwt/LOH-high, and HRwt/LOH-low. As shown in Fig. 2A, we found that overall survival for subjects with *BRCA2-mut* HGSOC was significantly better than HRwt/LOH-high (HR, 0.71; 95% CI, 0.57–0.87;  $p < 0.0001$ ) and HRwt/LOH-low subjects (HR, 0.59; 95% CI, 0.49–0.72;  $p < 0.0001$ ). Consistent with this observation, we also found that subjects with *BRCA2-mut* HGSOC had significantly better post-Carboplatin survival (Fig. 2B) compared to HRwt/LOH-high (HR, 0.74; 95% CI, 0.56–0.96;  $p = 0.022$ ) and HRwt/LOH-low subjects (HR, 0.49; 95% CI, 0.38–0.63;  $p < 0.000001$ ). Although *BRCA2-mut* subjects demonstrated longer median survival than *BRCA1-mut*, this did not reach statistical significance (HR, 1.05; 95% CI, 0.85–1.31;  $p = 0.65$ ). Similarly, *BRCA2-mut* subjects demonstrated longer post-Carboplatin survival compared to *BRCA1-mut*, but this also did not reach statistical significance (HR, 1.19; 95% CI, 0.90–1.57;  $p = 0.215$ ). These results are in line with a number of previous studies demonstrating better OS in HGSOC patients with mutations in *BRCA2* [9,15,16].

### 3.3. Genomic differences between *BRCA1-mt*, *BRCA2-mt* and HRWT HGSOC cohorts

In our cohort, the most common pathogenic mutations in *BRCA1* were frameshift mutations, of which the most common were E23fs and Q1756fs on the zinc finger domain and C-terminus domain, respectively (Fig. 3A). The most common mutation in *BRCA2* was also a frameshift mutations with the most common protein change being W1692fs in the RAD51 binding domain (Fig. 3B).

To better characterize the genomic heterogeneity of our cohort, we identified the most common molecular co-alterations such as other mutations and amplifications. We identified mutations in *TP53*, *NF1*, *RB1*, *CDK12*, *PIK3CA*, *KRAS*, *PPP2R1A*, *ATM*, *BRAF*, and *CHK2* as the most significantly altered co-occurring mutations (Fig. 4A). *TP53* is mutated in majority of the subjects in all groups as expected for the HGSOC subtype (*BRCA1-mut* vs *BRCA2-mut* vs HRwt/LOH-high vs HRwt/LOH-low: 96.9% vs 92.7% vs 96.8% vs 87.2%). *BRCA2-mut* HGSOC had the highest *NF1* mutation rate (13.1%) compared to *BRCA1-mut*, HRwt/LOH-high and HRwt/LOH-low (11.7%, 5.4%, 4.1%, respectively) while *BRCA1-mut* HGSOC had lowest mutation rates for *RB1* (2.6% vs 9.9% vs 10.7% vs 7.5%), *CDK12* (0.4% vs 0.7% vs 5.8% vs 0.8%) and *KRAS* (0.2% vs 1.7% vs 0.8% vs 4.7%) compared to *BRCA1-mut*, HRwt/LOH-high and HRwt/LOH-low. *BRCA1* and *BRCA2* mutations were mutually exclusive of mutations in *PPP2R1A*.

We observed amplification in *CCNE1*, *AKT2* and *ERBB2* (Fig. 4B). The distribution of these amplifications across the four patient groups is statistically significant (Fig. 4B, right panel). *BRCA1* and *BRCA2* mutations were associated with lower rates of amplification of *CCNE1* when compared to either the HRwt/LOH-high or HRwt/LOH-low cohorts respectively (1% vs 2.1% vs 9.4% vs 10.9%), *AKT2* (0.4% vs 0.7% vs 3.4% vs 3.7%), and *ERBB2* (0.4% vs 0.3% vs 3.2% vs 2%). Fig. 4C shows a mutual exclusivity plot demonstrating that *BRCA1/2* mutations are likely to co-occur with LOH but not with *CCNE1* amplification and that *CCNE1* amplification is most often correlated with HRwt HGSOC.

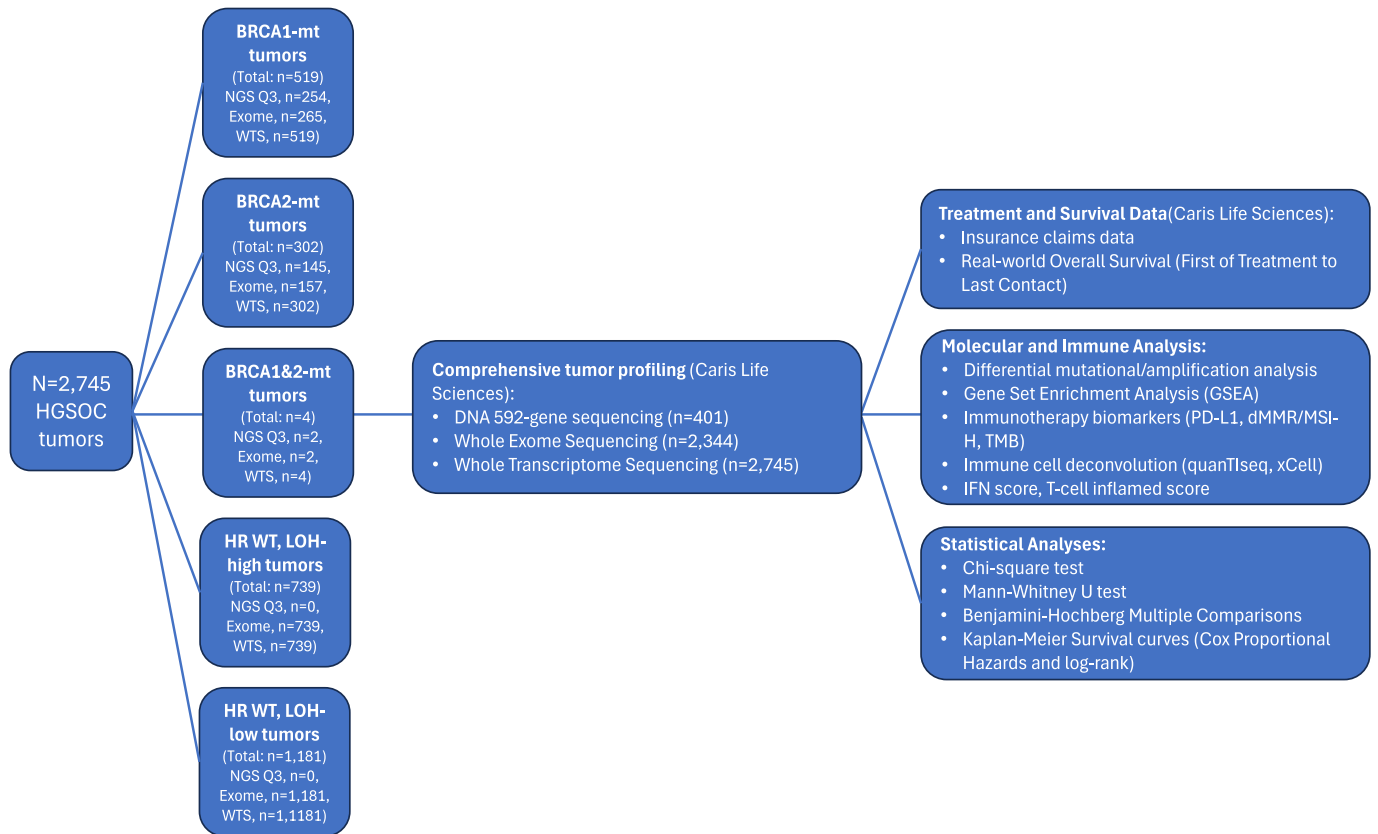


Fig. 1. Study flow chart. Flow chart showing approach in the comparative analysis of BRCA1-mut, BRCA2-mut, HRwt/LOH-high, and HRwt/LOH-low HGSOC.

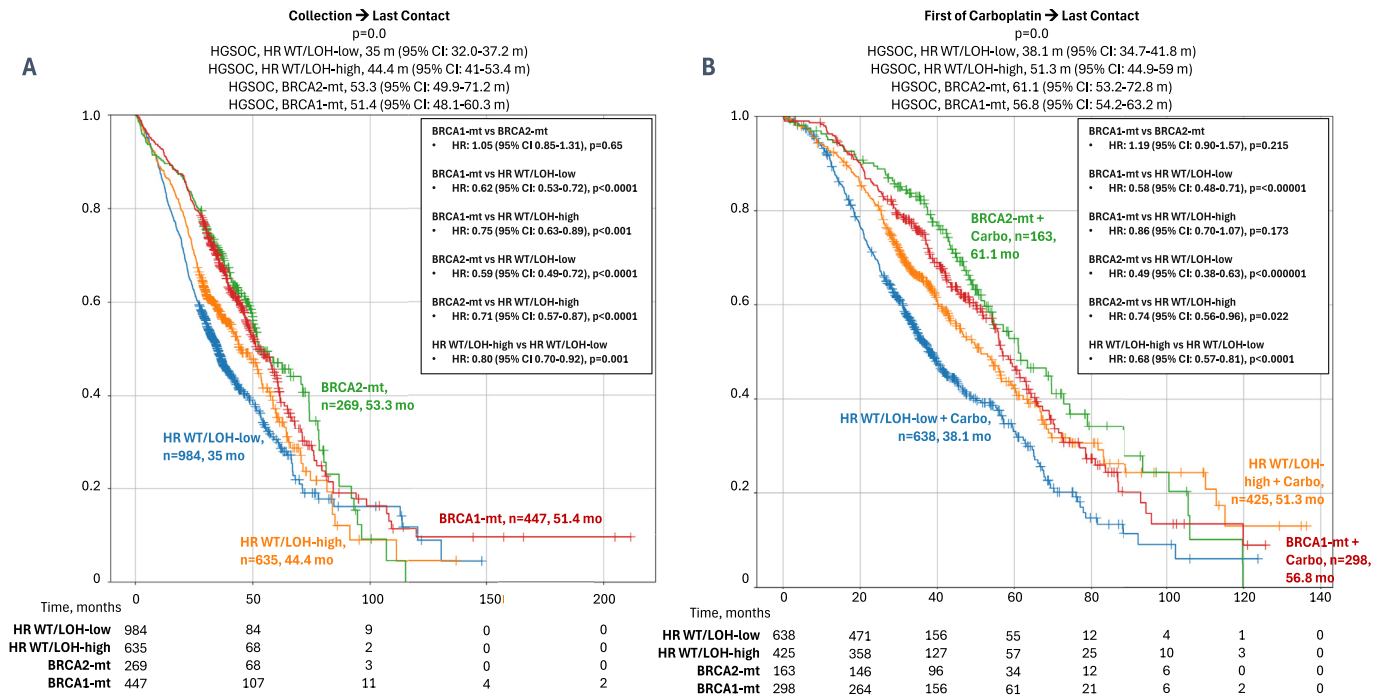
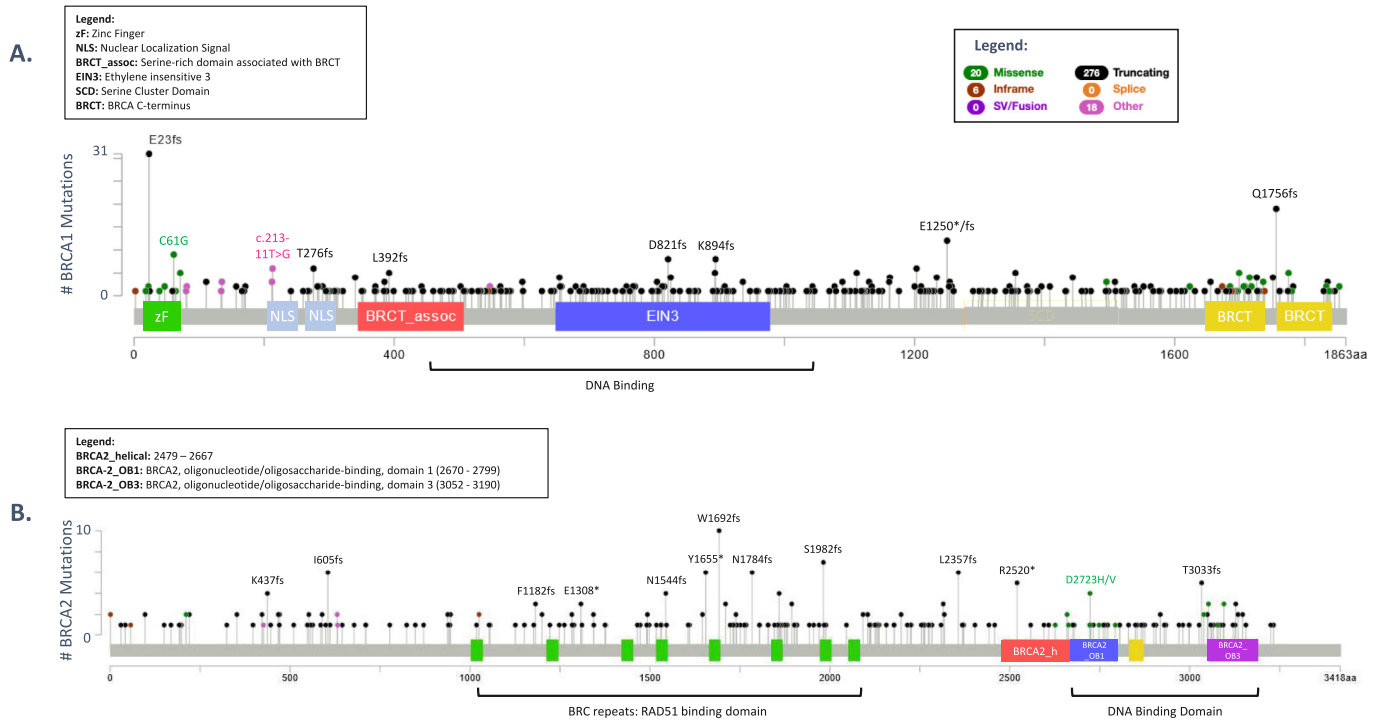
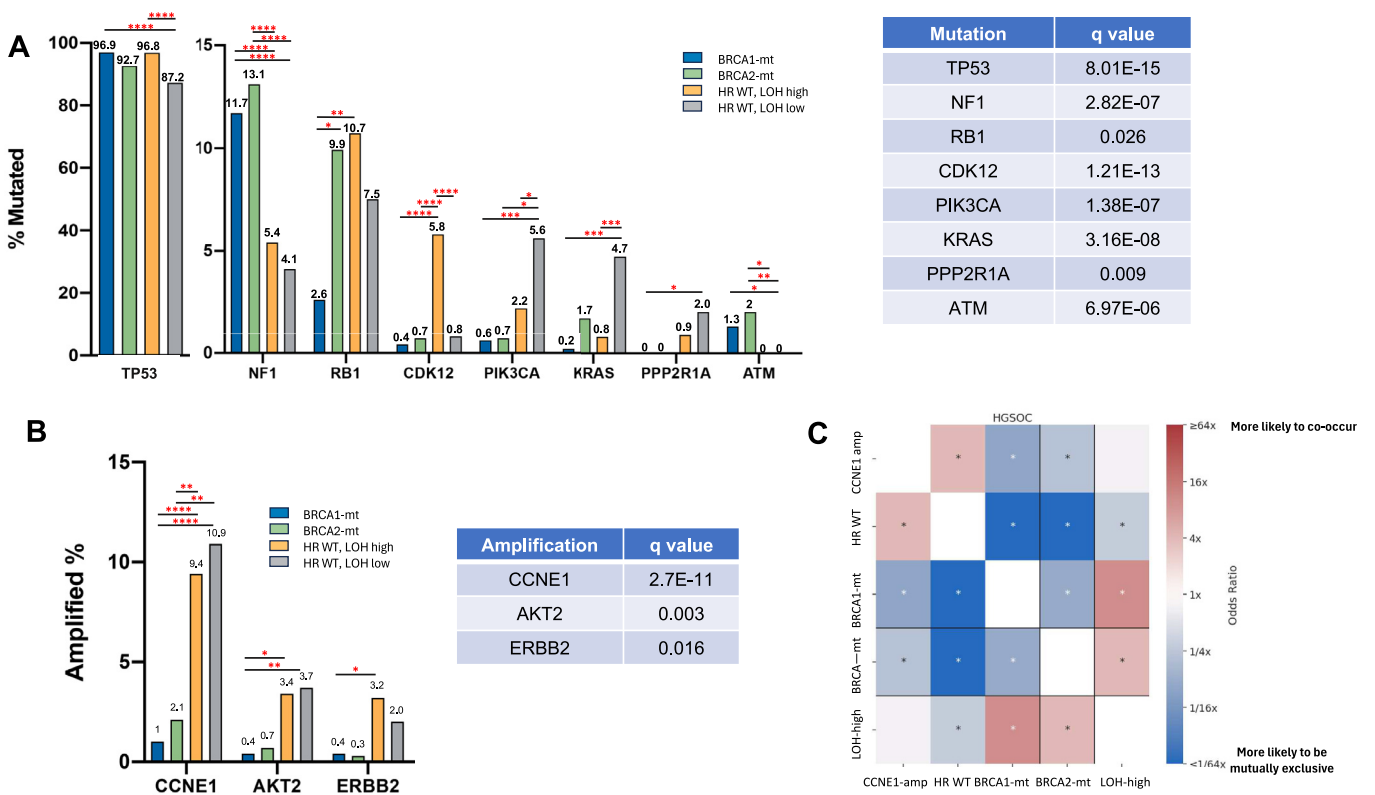


Fig. 2. BRCA2 mutations are associated with improved overall and post-Carboplatin survival compared to BRCA1-mut, HRwt/LOH-high, and HRwt/LOH-low HGSOC. A: Real-world overall survival calculated from time of tissue collection to last contact based on insurance claims data for molecularly defined cohorts: BRCA1-mut, BRCA2-mut, HRwt/LOH-high and HR wt/LOH-low HGSOC; B: Post-carboplatin survival calculated from time of first Carboplatin treatment to last contact for molecularly defined cohorts: BRCA1-mut, BRCA2-mut, HRwt/LOH-high and HRwt/LOH-low HGSOC. Cohort sizes, median survival in months and those at risk at each timepoint listed on figure.



**Fig. 3.** Lollipop plots of BRCA1 and BRCA2 mutations. Lollipop plots depict the distribution and types of pathogenic/likely pathogenic mutations present in BRCA1-mut (A) and BRCA2-mut (B) HGOC. DNA binding sites are also depicted. Different colored text/dots represent different types of mutations (listed in legend).



**Fig. 4.** Molecular co-alterations in BRCA1-mut, BRCA2-mut, HRwt/LOH-high and HR wt/LOH-low HGOC. A: Top co-altered genes ( $q < 0.05$ ) shown with individual group comparisons; B: Top co-amplified genes ( $q < 0.05$ ) shown; C: Mutual-exclusivity plot depicts genes that are more likely to co-occur (in red) and more likely to be mutually exclusive (blue) by odds ratio calculation. \* $q < 0.05$ , \*\* $q < 0.01$ , \*\*\* $q < 0.001$ , \*\*\*\* $q < 0.0001$ . (For interpretation of the references to color in this figure legend, the reader is referred to the web version of this article.)

### 3.4. Differentially regulated pathways in BRCA1-mt, BRCA2-mt and HR WT HGSOC

To identify molecular mechanisms that are distinct to each of the genomically-defined cohort, we performed GSEA analysis using 50 Hallmarks of Cancer Gene Sets and compared the 4 groups to each other. This resulted in 6 different comparisons (Fig. 5): BRCA1-mut vs BRCA2-mut; BRCA1-mut vs HRwt/LOH high; BRCA1-mut vs HRwt/LOH low; BRCA2-mut vs HRwt/LOH high; BRCA2-mut vs HRwt/LOH low and HRwt/LOH high vs HRwt/LOH low. Fig. 5 shows all gene sets with significant enrichment for each of the six comparisons performed. Given that our goal is to identify distinct molecular signatures in BRCA1-mut compared to BRCA2-mut HGSOC, we first focused our attention on this comparison and observed 29 enriched gene sets (Fig. 5A). Out of these 29 enriched gene sets, 8 were immune related (Fig. 5A, asterisks): TNF alpha signaling via NFkB (NES: 1.65, FDR 0.178); IFN gamma Response (NES: 1.60, FDR: 0.111); Complement (NES: 1.53, FDR 0.169); Inflammatory Response (NES: 1.52, FDR: 0.163); Allograft rejection (NES: 1.48, FDR 0.156); IFN alpha Response (NES: 1.46, FDR: 0.141); IL2/STAT5 Signaling (NES: 1.43, FDR: 0.171); and IL6/JAK/STAT3 Signaling (NES: 1.42, FDR: 0.163). Interestingly, except for TNF alpha signaling via NFkB, all of these gene sets remained enriched when BRCA1-mut was compared to HRwt/LOH high and HRwt/LOH low (Fig. 5B-C) suggesting differential regulation of immune response in BRCA1-mut tumors compared to the other genotypes. The other enriched gene sets (10/29) in BRCA1-mut vs BRCA2-mut HGSOC were metabolism related and included Reactive Oxygen Species (NES: 1.71, FDR: 0.133); Adipogenesis (NES: 1.64, FDR: 0.118); and Fatty acid metabolism (NES: 1.48, FDR: 0.158) as the top three metabolism-related gene sets (Fig. 5A). Although these metabolic pathways remained enriched when BRCA1-mut tumors were compared to HRwt/LOH-low HGSOC, we observed a more prominent enrichment of mTORC1 signaling and G2M checkpoint signals when these groups were compared (Fig. 5C). G2M checkpoint signals remained enriched when BRCA2-mut tumors were compared to the HRwt/LOH low (Fig. 5E) and when HRwt/LOH-

high were compared to HRwt/LOH-low (Fig. 5F). Taken together, these results show distinct molecular signatures between the different HGSOC genotypes and particularly suggest differential immune regulation in BRCA1-mut tumors.

### 3.5. Immune-oncology (IO) and immune checkpoint (IC) in BRCA1-mut, BRCA2-mut and HRwt HGSOC

Given the observed difference in immune-related pathways, we further characterized the tumor immune microenvironment and determined the levels of three common IO therapy-related biomarkers: PD-L1, TMB, and MSI (Fig. 6A, left panel). The distribution of PD-L1 and TMB across the four patient groups is significantly different between the genomically defined cohorts (Fig. 6A, right panel). PD-L1 (22c3) positivity was highest in BRCA1-mut tumors (6.4 %) and lowest in HR wt/LOH-low tumors (0.7 %). PD-L1 scores were statistically significant when BRCA1-mut tumors were compared to HRwt/LOH-low tumors but not when compared to BRCA2-mut or HRwt/LOH-high tumors (Fig. 6A). TMB was significantly higher in BRCA2-mut tumors (6.4 %) compared to the other genomically-defined HGSOC subsets (BRCA1-mut, 1.4 %; HRwt/LOH-high, 1.8 %; and HRwt/LOH-low, 0.7 %), suggesting enhanced antigenicity. BRCA2-mut tumors also had the greatest proportion of cancers classified as dMMR/MSI-H status (2.3 %; compared to BRCA1-mut 0.2 %; HRwt/LOH-high 0.8 %; and HRwt/LOH-low 0.3 %) although these differences were not statistically significant.

We also evaluated patterns of IC gene expression (CD80, CD86, CD274, PDCD1, PDCD1LG2, IDO1, LAG3, HAVCR2, CTLA4, IFNG) from bulk WTS data (Fig. 6B, top panel). The distribution of these IC biomarkers across the four patient groups is statistically significant (Fig. 6B, bottom panel). Specifically, we found that BRCA1-mut HGSOC were characterized by higher levels of IC gene expression when compared to HRwt/LOH-high and HRwt/LOH-low tumors. Except for IFN $\gamma$ , each of these IC genes evaluated were significantly higher in BRCA1-mut HGSOC than HRwt/LOH-high and HRwt/LOH-low tumors, but not significantly different when compared to BRCA2-mut HGSOC. Together,

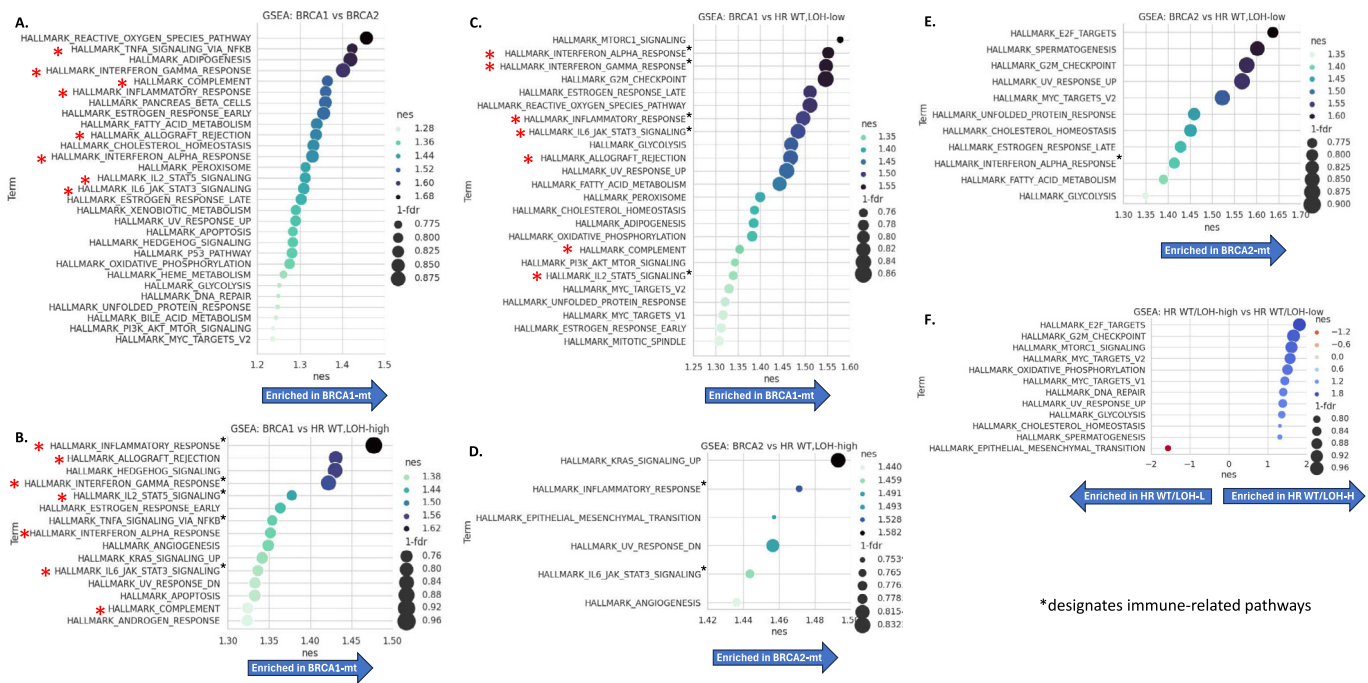
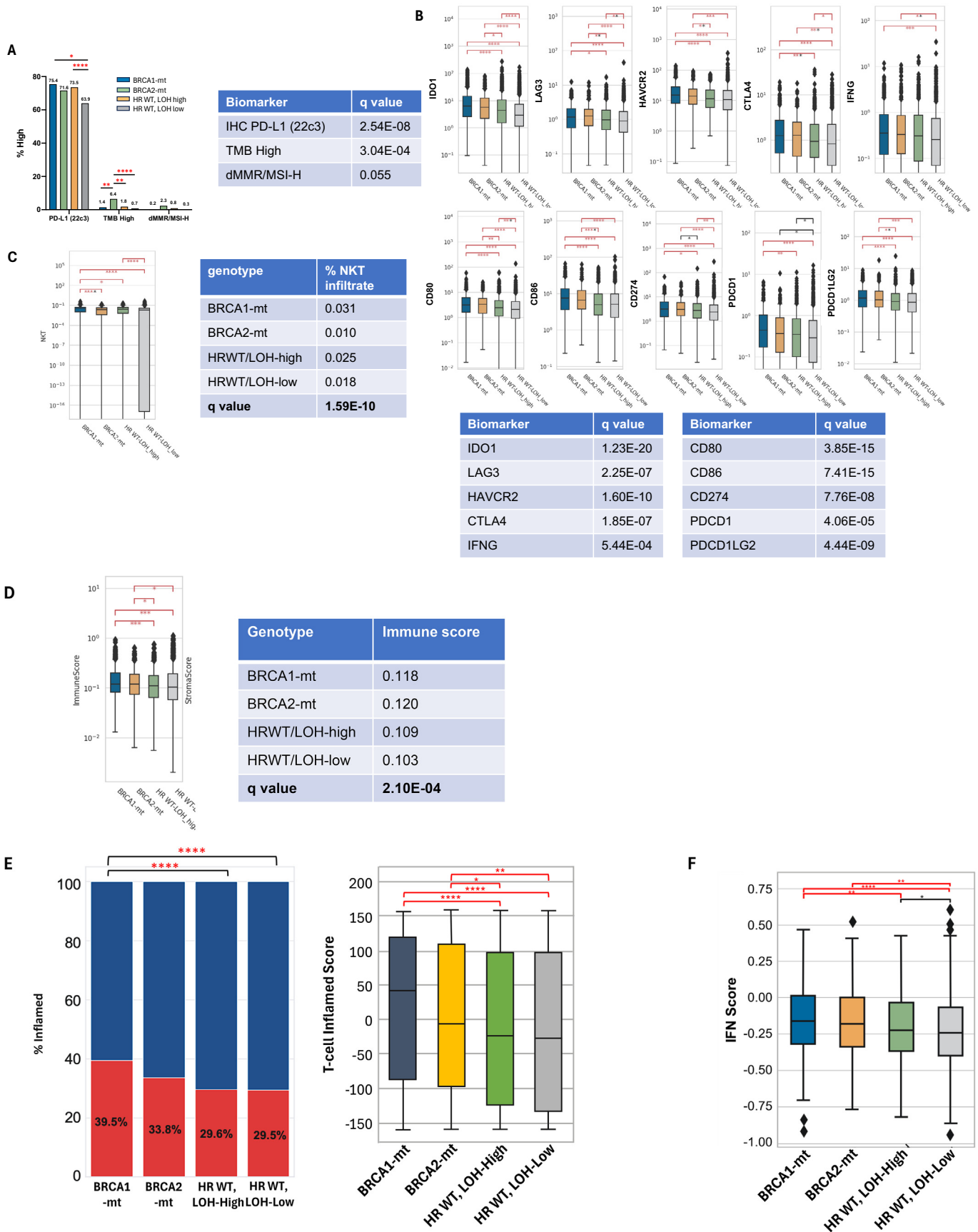


Fig. 5. Transcriptomic analysis in BRCA1-mut, BRCA2-mut, HRwt/LOH-high and HR wt/LOH-low HGSOC. GSEA using the Hallmarks of Cancer Pathways were conducted. Dotplots depict normalized enrichment score (NES) by color and False Discovery Rate (FDR) is depicted by size of dot. Arrows used to represent direction of enrichment. A: BRCA1-mut vs BRCA2-mut HGSOC tumors; B: BRCA1-mut vs HRwt/LOH-high HGSOC tumors; C: BRCA1-mut vs HR wt/LOH-low HGSOC tumors; D: BRCA2-mut vs HRwt/LOH-high HGSOC tumors; E: BRCA2-mut vs HRwt/LOH-low HGSOC tumors; and F: HRwt/LOH-high vs HRwt/LOH-low HGSOC tumors.



**Fig. 6.** Immune microenvironment of in BRCA1-mt, BRCA2-mt, HR WT/LOH-high and HR WT/LOH-low HGSOc. A: Immunotherapy-related biomarker (PD-L1 22c3, TMB High and dMMR/MSI-H) prevalence shown by molecularly defined group; B: Immune checkpoint gene expression (*CD80*, *CD86*, *CD274*, *PDCD1*, *PDCD1LG2*, *IFNG*, *IDO1*, *HAVCR2*, *LAG3*, *CTLA4*); C: Estimated NKT cell infiltration by quantIseq; D: Immune score E: T-cell inflamed score and F: IFN score shown. Individual comparisons shown on graph. \*q < 0.05, \*\*q < 0.01, \*\*\*q < 0.001, \*\*\*\*q < 0.0001.

these findings suggest that *BRCA1-mut* tumors are associated with a more tolerogenic immune microenvironment, whereas *BRCA2-mut* tumors exhibit higher antigenicity.

### 3.6. Immune microenvironment of *BRCA1-mt*, *BRCA2-mt* and HRwt HGSOc

To better characterize the immune phenotypes, we used xCell to determine the proportions of various tumor-infiltrating immune cell types potentially present in each genomically-defined subset of HGSOc. Comparing the four genomically defined groups, we found significant differences in the enrichment of 21 out of 34 analyzed immune cell types. These differentially enriched cell types were categorized into myeloid and lymphocyte groups, as shown in Supplemental Figs. 1 and 2 respectively. Within the myeloid population, macrophages, M1 macrophages, dendritic cells (DCs), activated DCs, plasmacytoid DCs, and mast cells exhibited significant differences in enrichment across the four groups (Supplemental Fig. 1). Notably, with the exception of DCs, these myeloid cell types were significantly more enriched in *BRCA1-mut* tumors compared to HRwt/LOH-high and HRwt/LOH-low tumors but did not show significant differences when compared to *BRCA2-mut* tumors.

Within the lymphoid population, several types—such as B cells, class-switched memory B cells, plasma cells, CD4+ memory T cells, CD4+ naïve T cells, CD8+ T cells, CD8+ central memory T cells (Tcm), CD8+ naïve T cells, T regulatory cells (Tregs), Th1, Th2, and NKT cells—exhibited significant differences in enrichment across the four cohorts (Supplemental Fig. 2). Particularly, CD4+ memory T cells were significantly more abundant in both *BRCA1-mut* and *BRCA2-mut* tumors compared to HRwt/LOH-high and HRwt/LOH-low tumors. However, no significant difference in CD4+ memory T cells was observed between *BRCA1-mut* and *BRCA2-mut* tumors (Supplemental Fig. 2). Remarkably, NKT cells were the only immune cell type to show a significant difference between *BRCA1-mut* and *BRCA2-mut* tumors, being more enriched in *BRCA1-mut* tumors (Fig. 6C).

All progenitor phenotypes—granulocyte-macrophage progenitors (GMP;  $p = 0.081$ ), hematopoietic stem cells (HSC;  $p = 2.75E^{-20}$ ), common lymphocyte progenitors (CLP;  $p = 9.66E^{-8}$ ), and common myeloid progenitors (CMP;  $p = 8.25E^{-5}$ )—demonstrated significant differences among the four groups. Overall immune scores were comparable between *BRCA1-mut* and *BRCA2-mut* tumors, both of which showed significantly higher scores compared to HRwt/LOH-high and HRwt/LOH-low tumors when analyzed independently (Fig. 6D).

Finally, we assessed T-cell inflamed and IFN scores. We found that tumors with pathogenic *BRCA1* mutations were significantly more likely to be classified as T-cell inflamed compared to HRwt/LOH-high and HRwt/LOH-low tumors (Fig. 6E, left panel). While *BRCA1-mut* tumors also exhibited a higher proportion of T-cell inflamed tumors compared to *BRCA2-mut* tumors (39.5 % vs. 33.8 %,  $p = 0.102$ ), this difference did not reach statistical significance. Both *BRCA1-mut* and *BRCA2-mut* tumors showed significantly higher T-cell inflamed scores compared to HRwt/LOH-high and HRwt/LOH-low tumors (Fig. 6E, right panel). However, the difference in T-cell inflamed scores between *BRCA1-mut* and *BRCA2-mut* tumors did not achieve statistical significance. Additionally, *BRCA1-mut* tumors had significantly higher IFN scores compared to HRwt/LOH-high and HRwt/LOH-low tumors, but not compared to *BRCA2-mut* tumors (Fig. 6F). Overall, these findings suggest that *BRCA1-mut* tumors are associated with a more inflamed tumor immune microenvironment.

## 4. Conclusion

In this study, we present the largest genomic and transcriptomic analysis of *BRCA1-mut* and *BRCA2-mut* HGSOc to date. Utilizing a unique clinicogenomic database, we identified immune regulation differences as the most notable distinguishing feature. Understanding the functional impact of pathogenic mutations in *BRCA1/2* and other genes involved in HR unveils several promising avenues for targeted therapies.

Insights from these studies can guide the development of novel treatments specifically for *BRCA1-mut* and *BRCA2-mut* HGSOc while also informing combinatorial strategies for HRwt tumors.

HGSOc are largely considered to be immunologically cold tumors characterized by low levels of immune infiltrates, reduced expression of IC molecules, and poor clinical response to IC inhibitors [17]. Our results reveal that compared to *BRCA2-mut* and HRwt tumors, *BRCA1-mut* tumors exhibit elevated levels of genes associated with activated T cells (higher T cell inflamed and IFN scores), while also overexpressing IC genes. This points to a tumor microenvironment that may be particularly responsive to IC inhibitors (e.g., anti-PD-1/PD-L1 or anti-CTLA-4), which aim to block these immune evasion pathways and restore T cell-mediated anti-tumor activity.

Although our results primarily underscore differences between *BRCA1-mut* tumors and HRwt tumors, two significant distinctions were observed between *BRCA1-mut* and *BRCA2-mut* HGSOc: an enrichment of NKT cells in *BRCA1-mut* tumors and higher TMB and MSI in *BRCA2-mut* tumors. These findings suggest that the type of immune infiltrate present within the tumor microenvironment may dictate, not only tumor progression, but also the response to therapy. Indeed, in a previous study we described that long term survival for ovarian cancer patients is associated with modifications in the immune tumor microenvironment in response to neoadjuvant chemotherapy [18]. The differences in the cellular component of the immune infiltration in *BRCA1-mut* and *BRCA2-mut* tumors observed in our current study may further help to better understand how specific patterns of immune infiltration ultimately determine ovarian cancer outcomes.

At least in part, patterns of immune infiltrates may be determined by the mutational burden present in a specific cancer. In general, HGSOc with *BRCA1* or *BRCA2* mutations generally exhibit higher TMB compared to *BRCA* WT tumors. Our findings build on this observation by clearly demonstrating that *BRCA2-mut* HGSOc have higher TMB and MSI compared to *BRCA1-mut* tumors. This contrasts with a previous report by Strickland et al. [19], which found no significant difference in neoantigen load between *BRCA1-mut* and *BRCA2-mut* tumors. Although there is a correlation between TMB and the likelihood of generating neoantigens, not all mutations necessarily contribute to neoantigen formation. As such this difference may be due to the types of mutations in the individual patient cohort.

We categorized HRwt tumors into LOH-low and LOH-high groups to examine LOH independently of *BRCA* mutations. In our HGSOc cohort, we identified 60 % as HRwt/LOH-low and 40 % as HRwt/LOH-high based on a cutoff of  $\geq 16$  %. Genomic LOH has been associated with OS and progression-free survival (PFS) in ovarian cancer, with high LOH considered to be a positive risk factor particularly in the context of response to PARPi and platinum based chemotherapy [20,21]. Our analysis revealed that LOH-low tumors have the poorest survival rates.

We also found HRwt/LOH-low tumors to harbor the highest level of CCNE1 amplification and that CCNE1 amplification and *BRCA* mutation are mutually exclusive. CCNE1 amplification is observed in a subset of HGSOc cases and is associated with tumor aggressiveness, increased chemotherapy resistance and poorer prognosis [22]. Higher levels of co-occurring mutations in *PIK3CA*, *KRAS*, *PP2R1A*, and *BRAF* were also observed in HRwt/LOH-low tumors, suggesting that these mutations could serve as potential therapeutic targets for these tumors with poor prognosis.

To the best of our knowledge, this study represents the analysis of the largest cohort of HGSOc patients with *BRCA1* and *BRCA2* mutations. However, as the CARIS CODEai database utilizes insurance claims data it has certain limitations, including limited follow-up data on overall survival (OS). Additionally, the database lacks verified staging and grading data, and some samples may not have been processed at the time of initial surgery. Future research validating the immune phenotype characterization using either flow cytometry or immunohistochemistry assays on both human samples and mouse models of *BRCA1* or *BRCA2* knockout cell lines will further elucidate our findings.

In conclusion, HRwt tumors, whether LOH-low or LOH-high, exhibit characteristics of “cold tumors,” with lower T cell inflamed and IFN scores compared to BRCA mutant tumors. Targeted therapies focusing on CCNE1, AKT2, and ERBB2 amplifications, or CDK12, PIK3CA, KRAS, and PPP2R1A mutations, may offer promising therapeutic strategies for these tumors. In contrast, BRCA1-mt and BRCA2-mt HGSOc are moderately immune reactive. The higher T cell inflamed score and PDL1 expression suggests that *BRCA1-mut* tumors may be more responsive to treatment strategies that incorporate immunotherapy.

### CRedit authorship contribution statement

**Ayesha B. Alvero:** Writing – review & editing, Writing – original draft, Methodology, Formal analysis, Conceptualization. **Sharon Wu:** Writing – review & editing, Writing – original draft, Visualization, Validation, Supervision, Software, Resources, Project administration, Methodology, Investigation, Formal analysis, Data curation, Conceptualization. **Alex Farrell:** Project administration, Methodology, Investigation, Formal analysis. **Seongho Kim:** Writing – review & editing, Methodology, Investigation, Formal analysis. **John J. Wallbillich:** Writing – review & editing, Methodology. **Ira Winer:** Writing – review & editing, Methodology. **Robert Morris:** Writing – review & editing, Methodology. **David Spetzler:** Writing – review & editing, Methodology. **Matthew L. Anderson:** Writing – review & editing, Methodology. **Alberto Puccini:** Writing – review & editing, Methodology. **Nathaniel L. Jones:** Writing – review & editing, Methodology. **Thomas J. Herzog:** Writing – review & editing, Methodology. **Premal H. Thaker:** Writing – review & editing, Methodology. **Gil Mor:** Writing – review & editing, Writing – original draft, Visualization, Methodology, Conceptualization. **Radhika P. Gogoi:** Writing – review & editing, Writing – original draft, Visualization, Supervision, Resources, Project administration, Methodology, Investigation, Formal analysis, Conceptualization.

### Declaration of competing interest

None.

### Appendix A. Supplementary data

Supplementary data to this article can be found online at <https://doi.org/10.1016/j.ygyno.2025.02.010>.

### References

- [1] L.Y. Li, Y.D. Guan, X.S. Chen, J.M. Yang, Y. Cheng, DNA repair pathways in Cancer therapy and resistance, *Front. Pharmacol.* 11 (2020), 629266.

- [2] F.J. Groelly, M. Fawkes, R.A. Dagg, A.N. Blackford, M. Tarsounas, Targeting DNA damage response pathways in cancer, *Nat. Rev. Cancer* 23 (2023) 78–94.
- [3] K.B. Kuchenbaecker, J.L. Hopper, D.R. Barnes, et al., Risks of breast, ovarian, and contralateral breast Cancer for BRCA1 and BRCA2 mutation carriers, *JAMA* 317 (2017) 2402–2416.
- [4] D.M. Hyman, Q. Zhou, A. Iasonos, et al., Improved survival for BRCA2-associated serous ovarian cancer compared with both BRCA-negative and BRCA1-associated serous ovarian cancer, *Cancer* 118 (2012) 3703–3709.
- [5] T. Pal, J. Permeth-Wey, J.A. Betts, et al., BRCA1 and BRCA2 mutations account for a large proportion of ovarian carcinoma cases, *Cancer* 104 (2005) 2807–2816.
- [6] H.A. Risch, J.R. McLaughlin, D.E. Cole, et al., Prevalence and penetrance of germline BRCA1 and BRCA2 mutations in a population series of 649 women with ovarian cancer, *Am. J. Hum. Genet.* 68 (2001) 700–710.
- [7] R. Roy, J. Chun, S.N. Powell, BRCA1 and BRCA2: different roles in a common pathway of genome protection, *Nat. Rev. Cancer* 12 (2011) 68–78.
- [8] S. Li, V. Silvestri, G. Leslie, et al., Cancer risks associated with BRCA1 and BRCA2 pathogenic variants, *J. Clin. Oncol.* 40 (2022) 1529–1541.
- [9] D. Yang, S. Khan, Y. Sun, et al., Association of BRCA1 and BRCA2 mutations with survival, chemotherapy sensitivity, and gene mutator phenotype in patients with ovarian cancer, *JAMA* 306 (2011) 1557–1565.
- [10] T. Pal, J. Permeth-Wey, R. Kapoor, A. Cantor, R. Sutphen, Improved survival in BRCA2 carriers with ovarian cancer, *Fam. Cancer* 6 (2007) 113–119.
- [11] R.L. Coleman, A.M. Oza, D. Lorusso, et al., Rucaparib maintenance treatment for recurrent ovarian carcinoma after response to platinum therapy (ARIEL3): a randomised, double-blind, placebo-controlled, phase 3 trial, *Lancet* 390 (2017) 1949–1961.
- [12] A. Subramanian, P. Tamayo, V.K. Mootha, et al., Gene set enrichment analysis: a knowledge-based approach for interpreting genome-wide expression profiles, *Proc. Natl. Acad. Sci. U. S. A.* 102 (2005) 15545–15550.
- [13] R. Bao, D. Stapor, J.J. Luke, Molecular correlates and therapeutic targets in T cell-inflamed versus non-T cell-inflamed tumors across cancer types, *Genome Med.* 12 (2020) 90.
- [14] M. Ayers, J. Lunceford, M. Nebozhyn, et al., IFN-gamma-related mRNA profile predicts clinical response to PD-1 blockade, *J. Clin. Invest.* 127 (2017) 2930–2940.
- [15] J.R. McLaughlin, B. Rosen, J. Moody, et al., Long-term ovarian cancer survival associated with mutation in BRCA1 or BRCA2, *J. Natl. Cancer Inst.* 105 (2013) 141–148.
- [16] K.L. Bolton, G. Chenevix-Trench, C. Goh, et al., Association between BRCA1 and BRCA2 mutations and survival in women with invasive epithelial ovarian cancer, *JAMA* 307 (2012) 382–390.
- [17] D. Fanale, A. Dimino, E. Pedone, et al., Prognostic and predictive role of tumor-infiltrating lymphocytes (TILs) in ovarian cancer, *Cancers (Basel)* (2022) 14.
- [18] N. Adzibolous, A.B. Alvero, R. Ali-Fehmi, et al., Immunological modifications following chemotherapy are associated with delayed recurrence of ovarian cancer, *Front. Immunol.* 14 (2023) 1204148.
- [19] K.C. Strickland, B.E. Howitt, S.A. Shukla, et al., Association and prognostic significance of BRCA1/2-mutation status with neoantigen load, number of tumor-infiltrating lymphocytes and expression of PD-1/PD-L1 in high grade serous ovarian cancer, *Oncotarget* 7 (2016) 13587–13598.
- [20] E.M. Swisher, T.T. Kwan, A.M. Oza, et al., Molecular and clinical determinants of response and resistance to rucaparib for recurrent ovarian cancer treatment in ARIEL2 (parts 1 and 2), *Nat. Commun.* 12 (2021) 2487.
- [21] D.M. O'Malley, A.M. Oza, D. Lorusso, et al., Clinical and molecular characteristics of ARIEL3 patients who derived exceptional benefit from rucaparib maintenance treatment for high-grade ovarian carcinoma, *Gynecol. Oncol.* 167 (2022) 404–413.
- [22] S. Bai, S.E. Taylor, M.A. Jamalruddin, et al., Targeting therapeutic resistance and multinucleate giant cells in CCNE1-amplified HR-proficient ovarian cancer, *Mol. Cancer Ther.* 21 (2022) 1473–1484.